

Template-Induced Screw Motions within an Aromatic Amide Foldamer Double Helix**

Yann Ferrand, Quan Gan, Brice Kauffmann, Hua Jiang,* and Ivan Huc*

Important steps have been made to control motion at the molecular scale in synthetic systems. Examples of elementary molecular motions such as rotations^[1] and translations^[2] have been reported, as well as combined motions such as coupled rotations,^[3] coupled translations,^[4] and springlike extensions.^[5] In addition, the direction of molecular movements can sometimes be controlled in translations (shuttling)^[6] and in rotations.^[7] Herein, we focus on a less-investigated motion, the screw motion, which consists of the linear combination of a rotation and a translation. We found that the sliding of two molecular tapes along one another within a double-helical duplex can be controlled by rodlike guests, so that the length of the duplex matches with the length of the guest (Figure 1 a).

We recently described the ability of some multiturn single-helical aromatic amide foldamers to wind around rodlike guests and form stable complexes in which the guest resides in the helix cavity.^[8] By analogy with rotaxanes, these complexes can be termed foldaxanes.^[9] When the rods have bulky residues at the termini, foldaxanes do not form by the threading of the rod into the helix cavity but by the unfolding/refolding of the helix around the rod. This creates a high kinetic barrier, owing to the high energy cost to unfold a helical aromatic oligoamide foldamer, as shown, for example, in quinolinecarboxamide oligomers.^[10] The unusual kinetic stability of the foldaxanes has allowed us to induce and observe shuttling of the helix between distinct stations along a dumbbell rod at timescales that are much shorter than the timescale of foldaxane dissociation. Foldaxane formation is

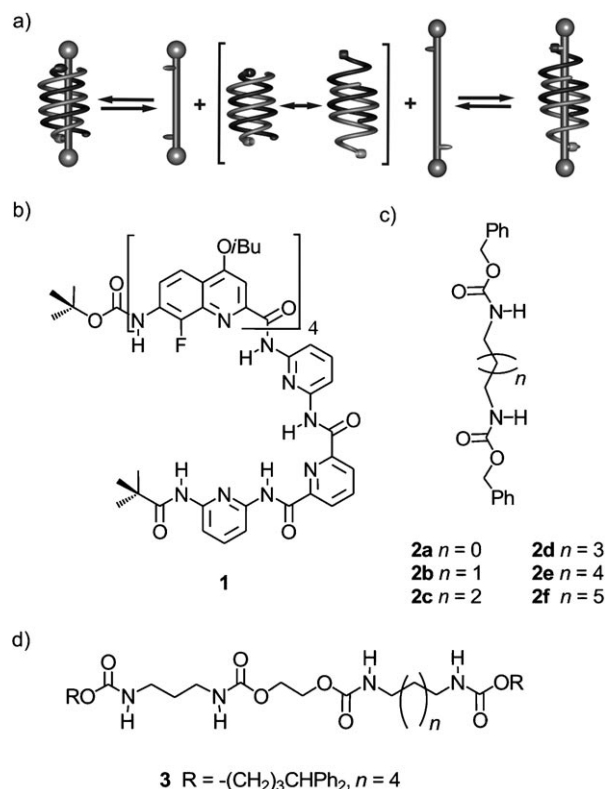


Figure 1. a) A schematic representation of the screw motion of the two strands of a molecular duplex, and of the trapping of screwed (left) and unscrewed (right) double helices upon binding to short and long rodlike guests, respectively. Hydrogen-bond acceptors (the sticks protruding from the rods) on the guests match with hydrogen-bond donors (small rings) at the ends of a double helix; b) the structure of helical aromatic oligoamide foldamer **1**; c) the structure of guests of various lengths, which possess carbonyl groups as hydrogen-bond acceptors; d) the structure of a guest having two distinct stations, a long one and a short one, to which a double helix can bind.

thermodynamically favored owing to intermolecular hydrogen bonds between binding sites, which are located at each extremity of the helix (namely 2,6-pyridinedicarboxamide hydrogen-bond donors), and anchor points on the rods (carbonyl hydrogen-bond acceptors).^[8] It follows that a strict match between helix and rod lengths is required to ensure foldaxane stability; the tolerance is typically one CH_2 unit of the rod.

Following this, we proposed that foldaxanes might form not only with aromatic oligoamide sequences that are folded as single helices, but also when they hybridize into double helices.^[5d,e,11] For example, sequences related to **1** (Figure 1 b) have been shown to hybridize into stable double-helical antiparallel duplexes.^[11,12] Because the double helix (**1**)₂

[*] Dr. Y. Ferrand, Q. Gan, Dr. I. Huc
Université de Bordeaux—CNRS UMR5248
Institut Européen de Chimie et Biologie
2 rue Robert Escarpit, 33607 Pessac (France)
E-mail: i.huc@iecb.u-bordeaux.fr

Dr. B. Kauffmann
Université de Bordeaux—CNRS UMS3033
Institut Européen de Chimie et Biologie
2 rue Robert Escarpit, 33607 Pessac (France)
Q. Gan, Prof. H. Jiang
Beijing National Laboratory for Molecular Sciences
CAS Key Laboratory of Photochemistry
Institute of Chemistry, Chinese Academy of Sciences
Beijing 100190 (China)
E-mail: hjjiang@iccas.ac.cn

[**] This work was supported by the CNRS, the Conseil Régional d'Aquitaine, an ANR grant (ANR-09-BLAN-0082-01), the Chinese Academy of Sciences, and the National Natural Science Foundation of China (20972164). We thank Axelle Grélaud for her assistance with NMR measurements.

Supporting information for this article is available on the WWW under <http://dx.doi.org/10.1002/anie.201101697>.

possesses two 2,6-pyridinedicarboxamide hydrogen-bond donors, that is one on each strand, we predicted that it might also bind to rodlike guests having carbonyl hydrogen-bond donors. Titrations between $(\mathbf{1})_2$ and $\mathbf{2a-f}$ (Figure 1c) in CDCl_3 were monitored by ^1H NMR spectroscopy and, in some cases, revealed the formation of a new species that was in slow exchange with $(\mathbf{1})_2$ on the NMR timescale (Figure 2a–c). Specifically, the longest ($\mathbf{2f}$) and shortest ($\mathbf{2a}$) rods do not form inclusion complexes, whereas rods of intermediate sizes $\mathbf{2b-e}$ do, with binding constants of 55, 20, 140, and 35 L mol^{-1} , respectively. These complexes all formed at rates too fast to monitor by ^1H NMR spectroscopy, as equilibrium is reached before the first ^1H NMR spectrum could be measured, which takes approximately 2 min. This process is faster than that previously observed for single-helical foldaxanes that are derived from longer aromatic amide sequences. Thus, to bind a rod of given length, two short strands appear to unwind and rewind faster than a long one.^[8]

The X-ray crystal structures of $(\mathbf{1})_2\mathbf{2b}$, $(\mathbf{1})_2\mathbf{2d}$, and $(\mathbf{1})_2\mathbf{2e}$ were obtained (Figure 3),^[13] and confirmed the stoichiometry, symmetry, and the structure of the double-helical foldaxanes, in agreement with the NMR titration data. In particular the crystal structures revealed: 1) the expected hydrogen bonds between the 2,6-pyridinedicarboxamide units and carbonyl groups on the rod, as observed for single-helical foldaxanes;^[8] 2) the antiparallel nature of the double helices;

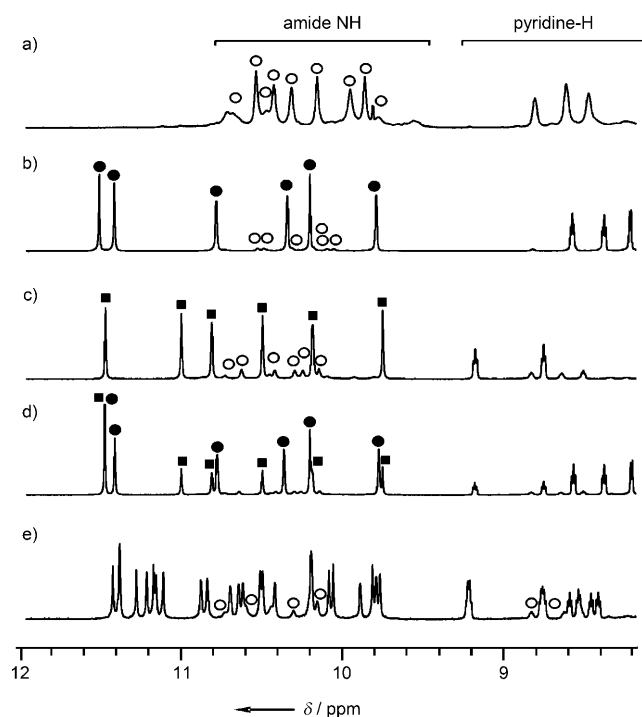


Figure 2. Part of the ^1H NMR spectra (700 MHz) showing the amide and some pyridine proton resonances of $(\mathbf{1})_2$ (8 mm) in CDCl_3 : a) at 25 °C in the absence of guest; b) at 0 °C in the presence of $\mathbf{2b}$ (10 equiv); c) at 0 °C in the presence of $\mathbf{2e}$ (10 equiv); d) at 0 °C in the presence of $\mathbf{2b}$ and $\mathbf{2e}$ (10 equiv each); e) at 0 °C in the presence of $\mathbf{3}$ (10 equiv). The signals of the starting double helix $(\mathbf{1})_2$ are marked with \circ , the signals of $(\mathbf{1})_2\mathbf{2b}$ with \bullet , and the signals of $(\mathbf{1})_2\mathbf{2e}$ with \blacksquare . Sharper NMR spectra could be recorded at 0 °C as shown in this figure.

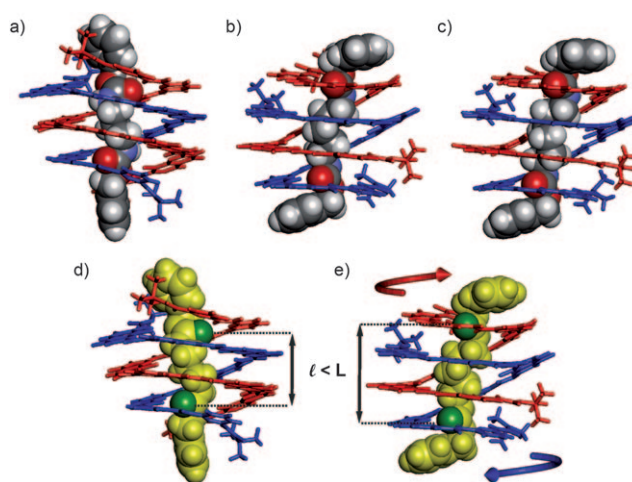


Figure 3. Solid-state structures of a) $(\mathbf{1})_2\mathbf{2b}$, b) $(\mathbf{1})_2\mathbf{2d}$, and c) $(\mathbf{1})_2\mathbf{2e}$. The antiparallel strands of $(\mathbf{1})_2$ are shown in red and blue (tube representation). Rodlike guests are shown in CPK (C gray, H white, O red, N light blue). Illustrations of the screw motion are shown in d) $(\mathbf{1})_2\mathbf{2b}$; and e) $(\mathbf{1})_2\mathbf{2d}$. Rods are in yellow CPK representations. The carbonyl oxygen atoms of the carbamate groups are shown in green. L and l represent the distance between the two pyridine clefts in each complex $(\mathbf{1})_2\mathbf{2b}$ and $(\mathbf{1})_2\mathbf{2d}$, and are equal to 6.8 Å and 9.0 Å, respectively. The red and blue arrows illustrate the screw-motion mechanism between complex $(\mathbf{1})_2\mathbf{2b}$ and $(\mathbf{1})_2\mathbf{2d}$. Isobutyl side chains and included solvent molecules have been omitted for clarity.

3) the C_2 -symmetrical structure of the complexes; 4) that the double-helix cavity accommodates the alkyl and carbamate moieties of the guest, but that the terminal benzyl groups are too large to be threaded through the helix, thus suggesting a helix unfolding/refolding mechanism of formation for the double-helical foldaxanes, as demonstrated for single-helical foldaxanes.^[8]

Unlike single-helical foldaxanes, double-helical foldaxanes feature a high tolerance with respect to guest length; $\mathbf{2e}$ is three CH_2 units longer than $\mathbf{2b}$, yet they have comparable affinities for $(\mathbf{1})_2$. In addition, the binding constants as a function of guest length do not follow a trend. A close-up look at the X-ray crystal structures shows that to accommodate $\mathbf{2b}$ or $\mathbf{2d}$, the two strands of $(\mathbf{1})_2$ undergo a relative screw motion of over a third of a turn to adjust the distance along the helix axis between the two 2,6-dicarboxamide units, and their angular orientation is perpendicular to the helix axis. The structure of $(\mathbf{1})_2\mathbf{2e}$ is almost superimposable on that of $(\mathbf{1})_2\mathbf{2d}$, except that the alkyl segment of the guest is compacted in the case of $\mathbf{2e}$ so as to accommodate its extra CH_2 unit, an effect which has been observed in other systems.^[14] In agreement with the solid-state structures, ^1H NMR analysis of the solutions showed that signals belonging to terminal functionalities of the strands, for example, the pivaloyl protons and some pyridine protons (see Figure S5 in the Supporting Information), consistently shift upfield when the guest is shortened, thus suggesting an increase of ring-current effects as would be expected when the two strands screw into one another. Screwing is also the mechanism by which these double helices are presumed to form from single-stranded precursors in the absence of a

rodlike guest.^[15] Here, it is the length of the guest that templates the extent of the relative screwing of the two strands within each duplex. The binding constants as a function of guest length do not follow a trend; this result is probably due to the fact that an adjustment in the distance between the 2,6-pyridinedicarboxamide units of the duplex is accompanied by a concomitant change in their angular orientation, therefore not allowing a perfect match for all guests.

A titration of (**1**)₂ with an equimolar mixture of **2b** and **2e** was then carried out, and produced a mixture of (**1**)₂⊃**2b** and (**1**)₂⊃**2e** in a 2:1 ratio (Figure 2d). Rotating-frame nuclear Overhauser effect 2D spectroscopy (ROESY) measurements (Figure S6) were recorded on this mixture and showed intense exchange peaks between the corresponding protons of the two complexes. Correlations were also observed between each foldaxane and the uncomplexed (free) double helix (**1**)₂. This experiment demonstrates that the double helix may dissociate from one rod and then reassociate with another rod having a different length. The net outcome of this exchange process is a screw or unscrew motion within the duplex, yet it does not proceed through correlated translations and rotations of the strands, but through an unwinding/rewinding mechanism.

This process was taken a step further by placing two helix binding stations of different lengths on a single rod. For this purpose, guest **3** was equipped with two binding stations equivalent to those of **2b** and **2e**. Upon titrating (**1**)₂ with a large excess of **3** the complex (**1**)₂⊃**3** forms, in which a single duplex binds to **3**. No measurable amount of the higher aggregate, in which two double helices are bound to **3**, was observed. As expected, the ¹H NMR spectrum of (**1**)₂⊃**3** revealed two sets of signals that corresponded to two isomers in which (**1**)₂ was positioned either on the long station or on the short station of **3** (Figure 2e). Neither of these two isomers has a symmetrical structure; the two strands of the duplex are inequivalent in each isomer (Figure 4a). Consequently, the ¹H NMR spectrum of (**1**)₂⊃**3** features four times as many signals as that of, for example, (**1**)₂⊃**2b** (Figure 2e and b). ROESY experiments on (**1**)₂⊃**3** in CDCl₃ solutions revealed that intense exchange takes place between the isomer in which (**1**)₂ is positioned on the long station of **3** and the one in which (**1**)₂ is positioned on the short station, while cross-peaks with traces of the free (**1**)₂ were very weak. As above, the net outcome of this exchange is a screw or an unscrew motion within (**1**)₂. Remarkably, ROESY data demonstrate that exchange and consequently the screw/unscrew motion, proceed through the shuttling of the duplex along the guest and not by a dissociation/association mechanism. If the latter would occur, each of the four signals of any given proton of the duplex would correlate with the three others (Figure 4c) because the positions on the strands would be randomized in the dissociation process. However, correlations show that any given proton of one isomer of (**1**)₂⊃**3** exchanges with a single proton of the other isomer (Figure 4b and d), consistent with the shuttling of the duplex along the rod, and the concomitant screw motion. Shuttling requires the disruption of hydrogen bonds between the rod and the duplex and the screw motion of the two strands into

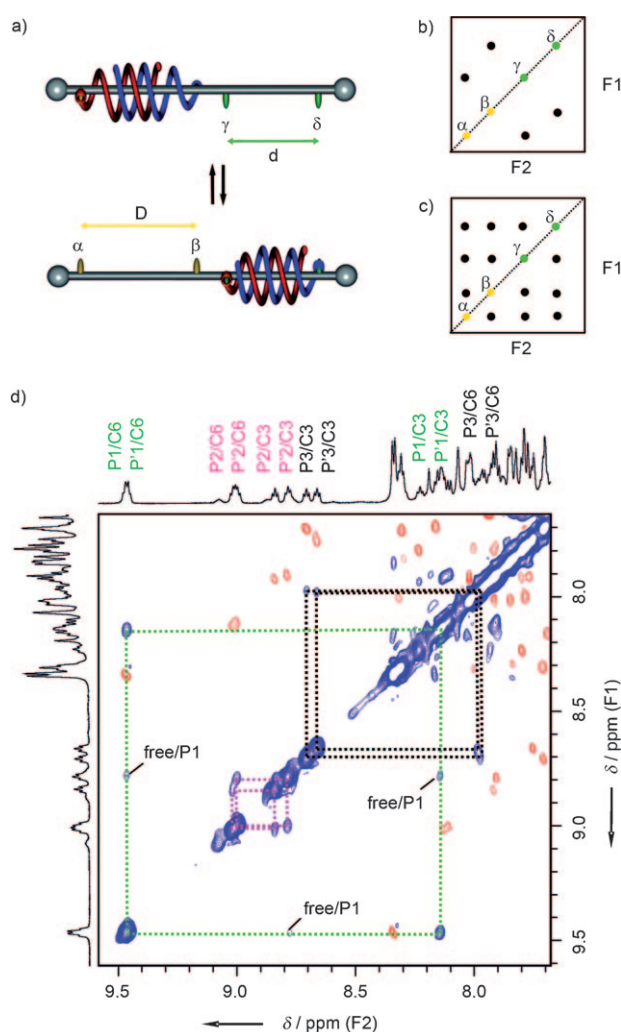


Figure 4. a) A schematic representation of the controlled screw/unscrew of a molecular duplex by its shuttling between two inequivalent stations of a rodlike guest. b) A schematic representation of the number of cross-peaks upon exchange of the duplex between the two inequivalent stations when exchange takes place by shuttling or c) by a dissociation/association mechanism. d) Expansion of the ¹H-¹H ROESY spectrum at 4 °C (700 MHz) of (**1**)₂⊃**3** (8 mM) recorded with 300 ms mixing time, thus showing that any given proton of one isomer of (**1**)₂⊃**3** exchanges with a single proton of the other isomer. NOE cross-peaks are observed in red whereas exchange peaks are seen in blue. P1, P2, P3 denote protons that belong to independent pyridine spin systems but have not been assigned to each pyridine ring in the sequence. C3 or C6 denotes the number (3 or 6) of CH₂ units in the alkyl chain of the station of the guest on which the double-helix resides.

one another, but these processes occur faster than foldaxane dissociation.

This work thus gave access to control over an unusual screw motion.^[16] Steps are now being made to increase its amplitude, to trigger it by an external stimulus, and to control the absolute sense of rotation in the right- or left-handed helices.

Received: March 9, 2011

Published online: June 29, 2011

Keywords: helical structures · rotaxanes · structure elucidation · supramolecular chemistry · X-ray diffraction

- [1] a) D. B. Amabilino, C. O. Dietrich-Buchecker, A. Livoreil, L. Pérez-García, J.-P. Sauvage, J. F. Stoddart, *J. Am. Chem. Soc.* **1996**, *118*, 3905–3913; b) T. C. Bedard, J. S. Moore, *J. Am. Chem. Soc.* **1995**, *117*, 10662–10671.
- [2] a) C.-F. Lee, D. A. Leigh, R. G. Pritchard, D. Schultz, S. J. Teat, G. A. Timco, R. E. P. Winpenney, *Nature* **2009**, *458*, 314–318; b) P. L. Anelli, N. Spencer, J. F. Stoddart, *J. Am. Chem. Soc.* **1991**, *113*, 5131–5133.
- [3] a) S. Hiraoka, E. Okuno, T. Tanaka, M. Shiro, M. Shionoya, *J. Am. Chem. Soc.* **2008**, *130*, 9089–9098; b) T. Muraoka, K. Kinbara, T. Aida, *Nature* **2006**, *440*, 512–515; c) J. Clayden, J. H. Pink, *Angew. Chem.* **1998**, *110*, 2040–2043; *Angew. Chem. Int. Ed.* **1998**, *37*, 1937–1939.
- [4] a) J. D. Badjic, V. Balzani, A. Credi, S. Silvi, J. F. Stoddart, *Science* **2004**, *303*, 1845–1849; b) M. C. Jiménez, C. Dietrich-Buchecker, J.-P. Sauvage, *Angew. Chem.* **2000**, *112*, 3422–3425; *Angew. Chem. Int. Ed.* **2000**, *39*, 3284–3287.
- [5] a) K. Miwa, Y. Furusho, E. Yashima, *Nat. Chem.* **2010**, *2*, 444–449; b) V. Percec, J. G. Rudick, M. Peterca, P. A. Heiney, *J. Am. Chem. Soc.* **2008**, *130*, 7503–7508; c) V. Maurizot, G. Linti, I. Huc, *Chem. Commun.* **2004**, 924–925; d) V. Berl, I. Huc, R. Khoury, M. J. Krische, J.-M. Lehn, *Nature* **2000**, *407*, 720–723; e) E. Berni, B. Kauffmann, C. Bao, J. Lefeuvre, D. M. Bassani, I. Huc, *Chem. Eur. J.* **2007**, *13*, 8463–8469.
- [6] a) M. R. Panman, P. Bodis, D. J. Shaw, B. H. Bakker, A. C. Newton, E. R. Kay, A. M. Brouwer, W. J. Buma, D. A. Leigh, S. Woutersen, *Science* **2010**, *328*, 1255–1258; b) V. Serreli, C.-F. Lee, E. R. Kay, D. A. Leigh, *Nature* **2007**, *445*, 523–527; c) J. E. Green, J. W. Choi, A. Boukai, Y. Bunimovich, E. Johnston-Halperin, E. DeIonno, Y. Luo, B. A. Sheriff, K. Xu, Y. S. Shin, H.-R. Tseng, J. F. Stoddart, J. R. Heath, *Nature* **2007**, *445*, 414–417.
- [7] a) N. Ruangsapichat, M. M. Pollard, S. R. Harutyunyan, B. L. Feringa, *Nat. Chem.* **2011**, *3*, 53–60; b) D. A. Leigh, J. K. Y. Wong, F. Dehez, F. Zerbetto, *Nature* **2003**, *424*, 174–179; c) T. R. Kelly, H. De Silva, R. A. Silva, *Nature* **1999**, *401*, 150–152; d) N. Koumura, R. W. J. Zijlstra, R. A. van Delden, N. Harada, B. L. Feringa, *Nature* **1999**, *401*, 152–155.
- [8] Q. Gan, Y. Ferrand, C. Bao, B. Kauffmann, A. Grélard, H. Jiang, I. Huc, *Science* **2011**, *331*, 6021.
- [9] Foldaxanes may be considered as a class of rotaxanes in which the ring is involved in at least one non-covalent bond (here intramolecular π - π stacking within the helix) and adopts a closed ring structure through a reversible folding process.
- [10] N. Delsuc, T. Kawanami, J. Lefeuvre, A. Shundo, H. Ihara, M. Takafuji, I. Huc, *ChemPhysChem* **2008**, *9*, 1882–1890.
- [11] Q. Gan, C. Bao, B. Kauffmann, A. Grélard, J. Xiang, S. Liu, I. Huc, H. Jiang, *Angew. Chem.* **2008**, *120*, 1739–1742; *Angew. Chem. Int. Ed.* **2008**, *47*, 1715–1718.
- [12] C. Bao, Q. Gan, B. Kauffmann, H. Jiang, I. Huc, *Chem. Eur. J.* **2009**, *15*, 11530–11536.
- [13] CCDC 816152 [(1) \rightarrow 2b], 816315[(1) \rightarrow 2d], and 816316[(1) \rightarrow 2e] contain the supplementary crystallographic data for this paper. These data can be obtained free of charge from The Cambridge Crystallographic Data Centre via www.ccdc.cam.ac.uk/data_request/cif.
- [14] a) D. Ajami, J. Rebek, Jr., *Nat. Chem.* **2009**, *1*, 87–90; b) L. Trembleau, J. Rebek, Jr., *Science* **2003**, *301*, 1219–1220.
- [15] A. Acocella, A. Venturini, F. Zerbetto, *J. Am. Chem. Soc.* **2004**, *126*, 2362–2367.
- [16] A screw motion has been proposed in the shuttling of a rotaxane around a peptidic helix; see: A. Moretto, I. Menegazzo, M. Crisma, E. J. Shotton, H. Nowell, S. Mammi, C. Toniolo, *Angew. Chem.* **2009**, *121*, 9148–9151; *Angew. Chem. Int. Ed.* **2009**, *48*, 8986–8989.